Earth and Planetary Science Letters 280 (2009) 229–235

Contents lists available at ScienceDirect

Earth and Planetary Science Letters

journal homepage: www.elsevier.com/locate/epsl

Weak mantle in NW India probed by geodetic measurements following the 2001 Bhuj earthquake

D.V. Chandrasekhar [a], Roland Bürgmann [b,*], C.D. Reddy [c], P.S. Sunil [c], David A. Schmidt [d]

[a] National Geophysical Research Institute, Hyderabad, India
[b] Department of Earth and Planetary Science, University of California, Berkeley, USA
[c] Indian Institute of Geomagnetism, Mumbai, India
[d] Department of Geological Sciences, University of Oregon, Eugene, USA

ARTICLE INFO

Article history:
Received 15 October 2008
Received in revised form 23 January 2009
Accepted 23 January 2009
Available online 26 February 2009

Editor: R.D. van der Hilst

Keywords:
lithospheric rheology
postseismic deformation
intraplate earthquakes
viscosity

ABSTRACT

Far-reaching transient surface deformation following the 2001 M_w 7.6 Bhuj intraplate earthquake in NW India reveals visco-elastic flow in the mantle with only modest contributions from crustal relaxation processes. The relatively rapid decay of GPS-measured deformation rates indicates increasing effective viscosities of the mantle from 3×10^{18} Pa s in the first 6 months to 2×10^{19} Pa s during the 6-year observation period, consistent with a time and stress-dependent rheology, such as power-law flow by dislocation creep. The observed data do not require relaxation of the lower crust over these time scales and indicate a lower bound of 10^{20} Pa s on its effective viscosity. The unusually low viscous strength of the mantle below the earthquake epicentral region may be the long-lasting result of thermal weakening by the late Cretaceous Deccan plume and may be responsible for the unusually active intraplate seismicity in the region.

1. Introduction

Transient crustal deformation induced by large earthquakes can be used to infer the rheology of the continental crust and the upper mantle (Pollitz, 1992; Tabei, 1989; Thatcher et al., 1980). Generally, these studies find that the elastically strong part of the continental crust is 15–30 km thick, that the lower crust has a higher viscosity than the uppermost mantle, and that the mantle asthenosphere has a low viscosity ($<5\times10^{19}$ Pa s) (Bürgmann and Dresen, 2008). However, all of the postseismic deformation transients considered to date are from active plate boundary zones with strongly thinned lithosphere (<60 km), and relatively hot and hydrated mantle asthenosphere. In contrast, studies of postglacial rebound in stable shield areas (Fennoscandia, North America) indicate an elastic plate thickness of ~100 km overlying a high viscosity substratum ($>10^{20}$ Pa s) (Haskell, 1935; Milne et al., 2001). The Bhuj earthquake of January 26, 2001 in Kachchh, India is the largest event (Mw 7.6) in the last 50 years in a continental shield region and provides a unique opportunity to probe the rheology of the deep lithosphere in an intraplate region. We compare GPS, InSAR and gravity measurements to models of postseismic deformation caused by the earthquake to assess the viscous strength of the lower crust and upper mantle.

The M_w 7.6 Bhuj earthquake of January 26, 2001 in Kachchh was the most devastating earthquake to strike the Indian shield in its recorded history. The event and the nearby, similarly-sized 1819 Allah-Bund earthquake reactivated E–W trending Precambrian normal faults. The faults were also active during a rifting phase in Mesozoic time and subsequently reversed due to N–S compression associated with the collision of India with Eurasia (Biswas, 1987) and thus have steeper dips compared to usual thrust faults. This seismically active intraplate region lies >300 km from the nearest active boundary of the Indian plate.

2. Postseismic GPS, InSAR and gravity data

Time series of GPS-measured surface displacements document transient deformation during 6 years following the Bhuj earthquake. We update and expand on initial results from this network published by Reddy and Sunil (2008) who provide further detail on the GPS observations and analysis. Time series of positions of each site (shown in Fig. 1) in the well-determined International Terrestrial Reference Frame (ITRF2000) are obtained from the combined quasi-observations. Fig. 2 and Table S1 provide relative position time series from February 2001 to January 2007 of each site with respect to a station at Ahmedabad (AHMD). The time series show the decaying nature of the postseismic motions with total displacement of as much as 29 mm during the observation period. The decay of the postseismic displacements are well represented by a logarithmic function $a' + b' \log(t)$,

* Corresponding author. Tel.: +1 510 643 9545; fax: +1 510 643 9980.
E-mail addresses: go4sekhar@yahoo.com (D.V. Chandrasekhar), burgmann@seismo.berkeley.edu (R. Bürgmann), cdreddy@iigs.iigm.res.in (C.D. Reddy), sunilps@iigs.iigm.res.in (P.S. Sunil), das@uorogen.edu (D.A. Schmidt).

0012-821X/$ – see front matter © 2009 Elsevier B.V. All rights reserved.
doi:10.1016/j.epsl.2009.01.039

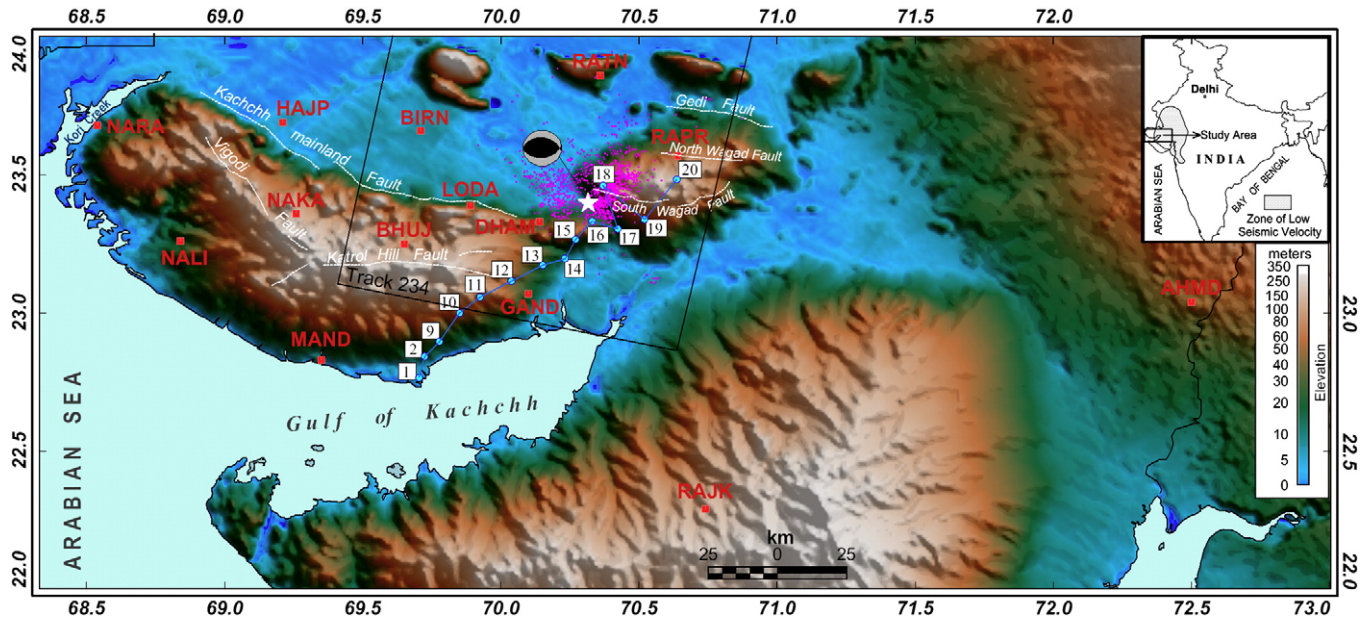

Fig. 1. Seismotectonic setting of the Bhuj earthquake. The location of GPS sites is annotated in red and stations occupied for repeat gravity observation along a profile are numbered. Pink dots indicate the aftershock distribution (Negishi et al., 2002). Color shaded topography is from a 90-m DEM obtained by the shuttle radar topography mission (SRTM). The coseismic rupture is located near the center of the aftershock distribution. The black box indicates the spatial coverage of the ERS-satellite track 234 InSAR frame. (For interpretation of the references to colour in this figure legend, the reader is referred to the web version of this article.)

where t is the time (yr) and a′ and b′ are constants to fit the displacement time series (Fig. 2). As there is some scatter about the best-fit curve and to interpolate between the sparse observation epochs, we used the logarithmic curve-fit values to estimate time-dependent total displacements at each site (Fig. 2). Other functional forms could provide equally good fits to the observations and the choice of a logarithmic function does not imply a particular relaxation process. In our modeling, we compare the model predictions to these cumulative motions over various time intervals. Fig. 3 presents the total displacements of our GPS stations with respect to AHMD for 6 months, 1 year, 2 years and 6 years after the Bhuj earthquake.

In addition to the GPS time series, we consider a single, postseismic SAR interferogram over Gujarat collected by the ERS-2 satellite along descending track 234. Unfortunately, the failure of gyroscopes on the ERS-2 spacecraft in January of 2001 results in there being only a single interferogram which spans the postseismic period from Feb. 14, 2002 to Feb. 19, 2004 (Schmidt and Bürgmann, 2006). In general, InSAR coherence is limited to the isolated highlands as the region is characterized by seasonal flooding in the lowlands. Topographically-correlated atmospheric artifacts dominate regions of the interferogram, further complicating the interpretation of the data. After flattening the scene, no obvious deformation signal is evident in the InSAR data (Fig. 5).

Gravity measurements were carried out along a profile in 2004 and 2007 with reference to a first observation in November of 2001 (Chandrasekhar et al., 2004) using a CG-5 gravimeter. Locations of the profile and stations are shown in Fig. 1 and gravity change values are listed in Table S2. Fig. 6 shows the observed gravity-change data with a depression of −0.1 mGal towards the southwest of the epicenter, followed by a gradual rise up to 0.05 mGal over the epicentral region.

3. Postseismic deformation models and results

The broadly distributed nature of the postseismic deformation field suggests a deeply buried source of transient deformation and thus we primarily consider models of viscous relaxation in our investigation. However, we also explore possible contributions from poroelastic rebound and afterslip. To calculate the viscoelastic postseismic deformation we adopt the earthquake source parameterization of Antolik and Dreger (2003), which is also consistent with geodetic constraints on the rupture (Chandrasekhar et al., 2004; Schmidt and Bürgmann, 2006; Wallace et al., 2006). The location of the rupture is shown in Fig. 3. Strike, dip, rake, and seismic moment are 82°, 51°, 77°, and 1.6×10^{20} Nm, respectively. The model rupture is 40 km long and 10–32 km deep. The slip distribution of Antolik and Dreger (2003) is simplified by compacting the slip distribution with a larger amount of slip (8.2 m) confined to the center (25×15 km^2) and less slip (1.7 m) on the surrounding part (Fig. S1).

We calculate postseismic deformation using VISCO1D (Pollitz, 1997), which is based on the normal mode representation of deformation in a layered spherical Earth with elastic-viscoelastic coupling, including the effects of compressibility and gravitational coupling. We consider a simple layered Earth model consisting of an elastic plate overlying a viscoelastic substrate as shown in Fig. S2. The free model parameters are the thickness H_p of the elastic plate and the viscosity η_a of the viscoelastic material below. We calculate postseismic cumulative displacements spanning 6 months to 6 years at each GPS site and calculate the root mean-square error (RMS) between the observed (log-fit) and predicted motions for each time period. We varied the plate thickness and viscosity parameters in the range of 25–50 km and 10^{17}–10^{21} Pa s at 1 km and 0.1 Pa s intervals, respectively (Fig. 3).

We determine parameters of the viscoelastic structure that minimize the misfit with the observed data using a forward modeling approach over a range of model parameters (Fig. 3). The minimum misfit is found at $H_p = \sim34$ km for all time periods considered, which is close to the local crustal thickness inferred from seismic data (Sarkar et al., 2001). This suggests that the elastic plate and the viscoelastic half space of this model are coincident with the crust and the upper mantle, respectively. Optimal effective mantle viscosities increase with time from $\eta_a = 3\times10^{18}$ Pa s for the first 6-month period to 2×10^{19} Pa s, if displacements for the full 6 years are considered (see Fig. S3). The systematic increase of the estimated effective viscosity with time suggests a time-dependent rheology, such as power-law flow by dislocation creep or transient creep. We note that far-field sites to the west appear to be systematically under-predicted by our models. This may suggest the effect of further decreasing viscosities at greater depth; however, we did not further explore more complex layered models.

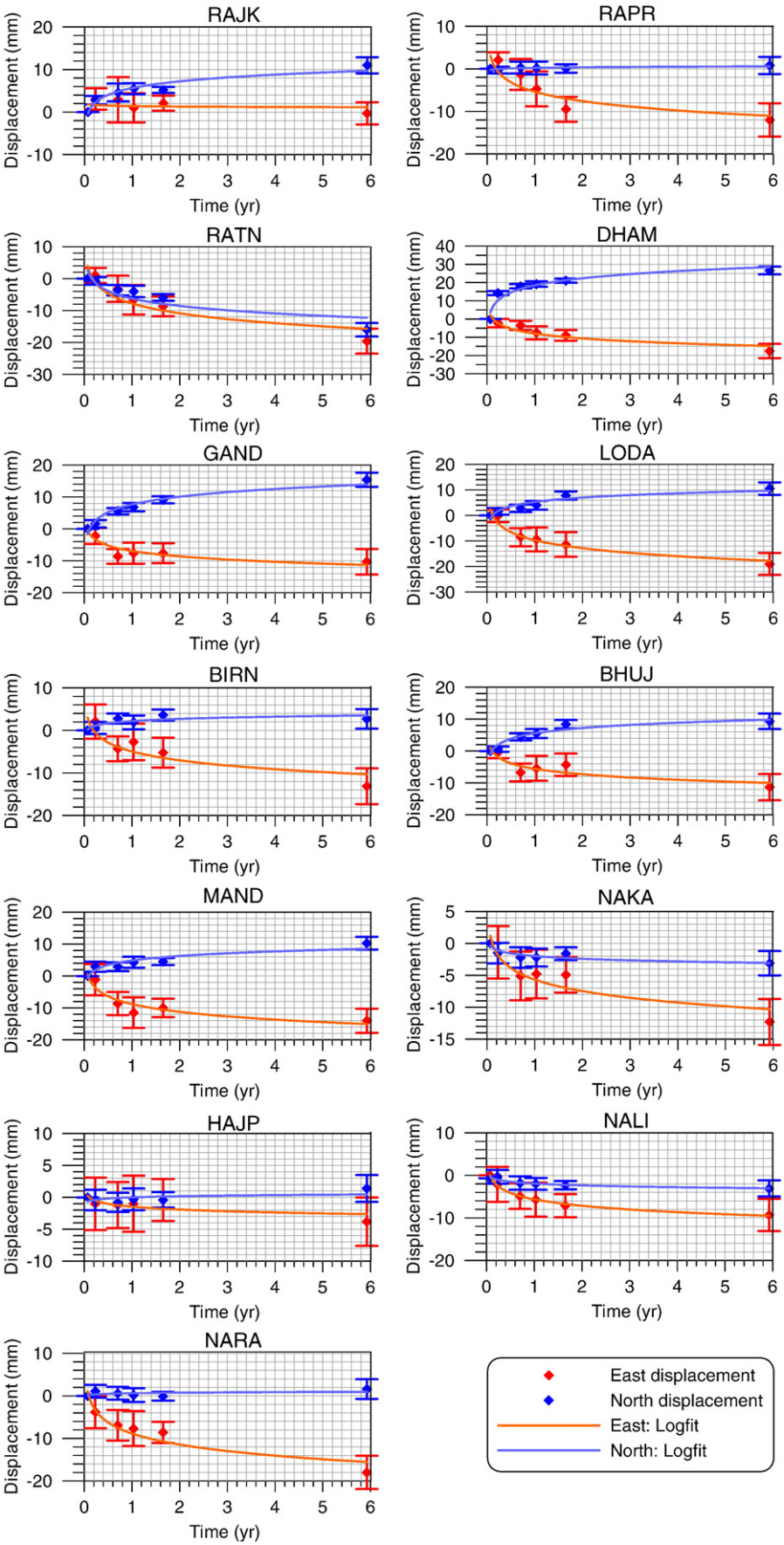

Fig. 2. East and North displacements of 13 GPS sites plotted with respect to AHMD site (see Fig. 1 for location) as a function of time following the Bhuj earthquake. The error bars represent one standard deviation on either side of the plotted point. Logarithmic fits to the data for time (yr) are shown by the red and blue color curves. (For interpretation of the references to colour in this figure legend, the reader is referred to the web version of this article.)

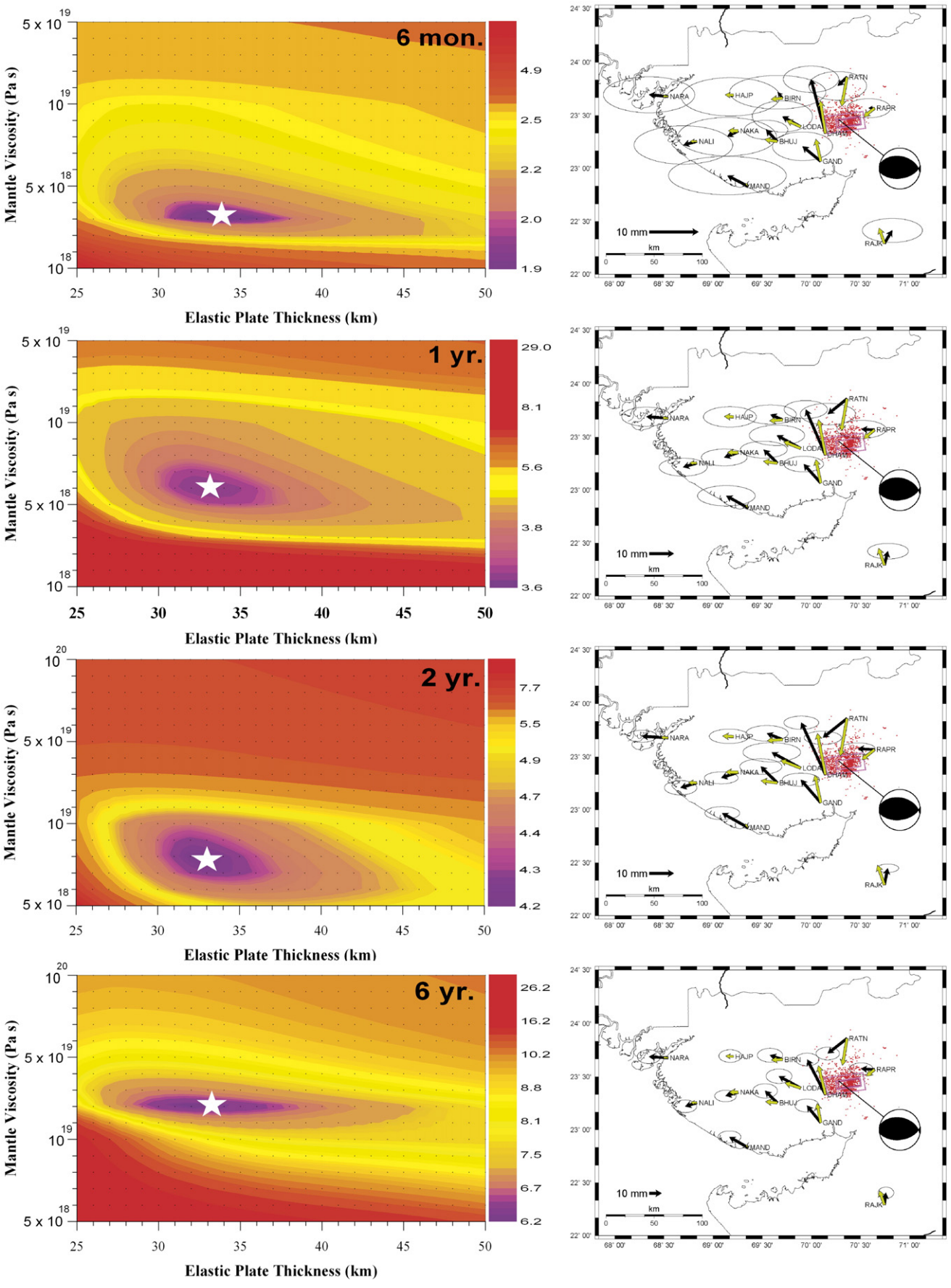

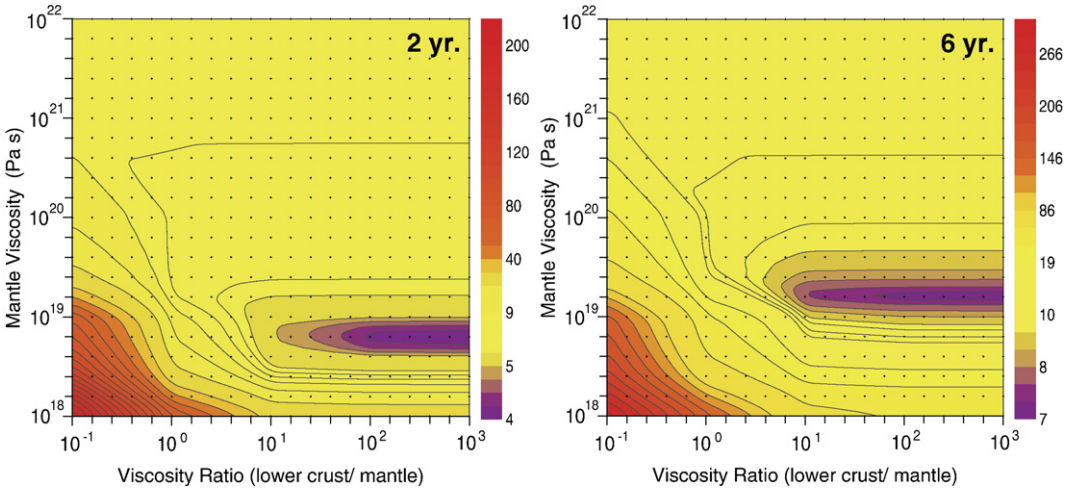

Fig. 4. The RMS misfit between the calculated and the observed horizontal displacements for 2 years and 6 years for the three-layer Earth model, which allows for viscous flow in the lower crust between 20 and 34-km depth. The RMS misfit is shown as a function of mantle viscosity (η_{lm}) and lower crust-to-mantle viscosity ratio ($\eta_{\mathrm{lc}}/\eta_{\mathrm{m}}$).

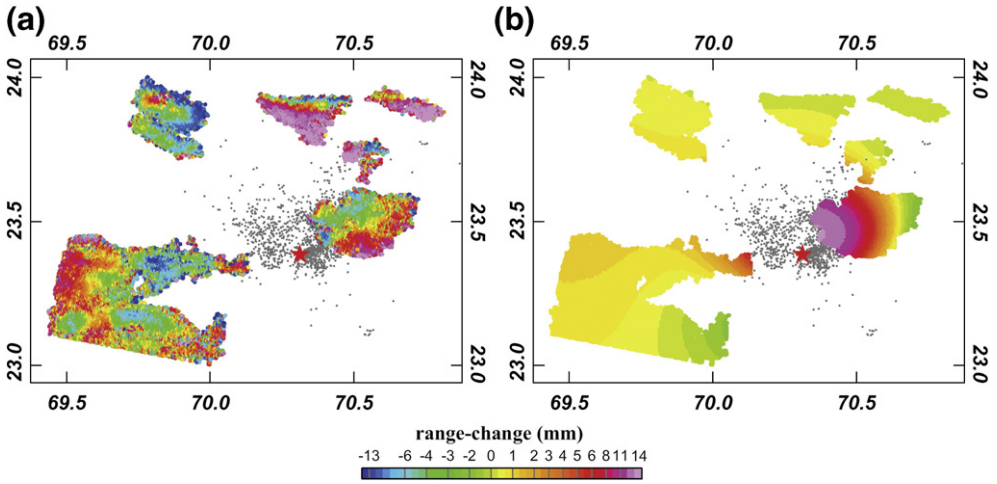

Fig. 5. The postseismic interferogram (left panel) with a perpendicular baseline of 300 m shows the observed range change from February 2002 to February 2004. Positive range-change corresponds to subsidence if all deformation is vertical. The right panel shows the synthetic postseismic range change computed using the visco-elastic model with a viscosity of 2×10^{19} Pa s obtained from the horizontal GPS motions during this time span. Red star and gray dots indicate the Bhuj mainshock and aftershocks (Negishi et al., 2002). (For interpretation of the references to colour in this figure legend, the reader is referred to the web version of this article.)

We examined the change of the best-fit effective viscosity of the asthenosphere for coseismic rupture models with higher moment magnitudes, given that some teleseismic moment estimates are as high as 3.6×10^{20} Nm (Wesnousky et al., 2001). An increase of the coseismic moment of the rupture by 1.5 times raises the effective viscosity estimates by 30–50% for the different time intervals considered. We also estimate the viscosity of a 15-km-thick lower crustal layer separate from the upper mantle (Fig. S3). The misfit plot (see Fig. 4) suggests that the observed data do not require relaxation of the lower crust and indicate a lower bound of 10^{20} Pa s on its effective viscosity over the time-scales of our observations.

Poroelastic rebound and afterslip often contribute to postseismic deformation transients. We test for the contribution of pore-fluid flow in response to mainshock induced pore-pressure changes to the observed deformation. Using a typical Poisson's ratio yield (0.05) between drained and undrained materials (Jónsson et al., 2003; Peltzer et al., 1996), we find a small contribution to the near-field horizontal deformation and very small eastward motions at most of the GPS sites, which were observed to move to the west (Fig. S4). Complete poroelastic rebound also predicts a zone of subsidence of as much as 65 mm localized over the buried coseismic rupture. We also consider simple elastic dislocation models (Okada, 1985) of afterslip up-dip, on and down-dip of the earthquake rupture, respectively (Fig. S5). Slip is assumed to be uniform on a rectangular dislocation with the same rake as the earthquake. A notable feature of the early displacement not captured well by our viscoelastic models is the rapid northward motion of station DHAM, located just to the south of the south-dipping rupture. Only shallow afterslip produces a sense of motion consistent with that observed at DHAM. None of the afterslip models that we explored produced the observed pattern or magnitude of motions across the western half of the GPS network. This is consistent with the results of Nishimura and Thatcher (2003), who demonstrated for the case of the post-1959 Hebgen Lake, USA, normal-faulting earthquake that the transient deformation produced by viscous relaxation and afterslip are distinctly different.

We compare the predicted deformation from our GPS-derived viscous relaxation model to the InSAR and gravity data. We calculate

Fig. 3. Model results. The RMS misfit between the calculated and observed horizontal displacements as a function of elastic plate thickness (H_{p}) and asthenosphere viscosity (η_{a}) for the two-layer Earth model as a function of time since the earthquake. The black dots indicate the model run points and the star marks the best-fit displacement model with the least RMS error value, whose best-fit horizontal displacements are plotted adjacent to the misfit plot. Vectors in black denote the observed displacement tipped with 95% confidence ellipses and yellow arrows are the calculated model displacements. (For interpretation of the references to colour in this figure legend, the reader is referred to the web version of this article.)

the range-change pattern from relaxation of a 2×10^{19} Pa s mantle corresponding to the 2002–2004 period spanned by the interferogram (Fig. 5). The model predicts a broadly distributed depression with subsidence of ~13 mm centered across the central epicentral region, which uplifted by more than 1 m during the earthquake (Schmidt and Bürgmann, 2006; Chandrasekhar et al., 2004). We suspect that either the InSAR data do not resolve a deformation signal or that shallow afterslip or groundwater level changes contribute to the near-field deformation.

The synthetic gravity field changes calculated for 2001–2004 (with an upper-mantle viscosity of 2×10^{19} Pa s estimated from the GPS displacements during this time span) and 2001–2007 (5×10^{19} Pas) match the spatial pattern of the observed gravity changes, but somewhat overpredict the gravity changes over the epicentral region (Fig. 6). Station 18, which is located immediately above the coseismic rupture and experienced the largest coseismic uplift and gravity reduction, has a large negative postseismic gravity change. This could be an indication of shallow afterslip, but the gravity data may also be affected by changes in the depth to the water table in the sedimentary terrain (Chandrasekhar et al., 2004).

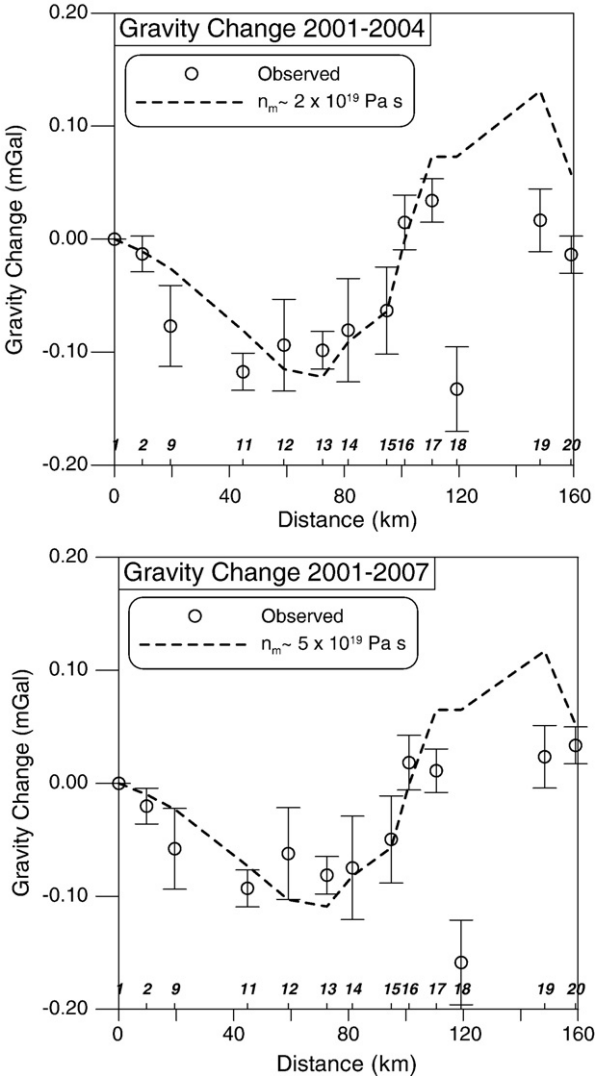

Fig. 6. The observed and predicted postseismic gravity changes for the 2001–2004 and 2001–2007 observations (Chandrasekhar et al., 2004). The predicted gravity changes are calculated using the viscoelastic relaxation model with the viscosities indicated in the legend. The error bars represent one standard deviation. Station locations are shown in Fig. 1, and coordinates and gravity change values are listed in Table S2.

4. Discussion and conclusions

The estimated first-order viscoelastic structure deduced from postseismic surface deformation measurements following the 2001 Bhuj earthquake consists of an elastic plate whose thickness is ~34 km and an underlying viscoelastic asthenosphere whose effective viscosity is 2×10^{19} Pa s, during the 6-year observation period. Modest, shallow afterslip may have contributed to the near-field GPS, InSAR and gravity changes. The observed far-field postseismic deformation field can be quite uniquely attributed to deep viscous flow, as deformation from poroelastic rebound or afterslip on or below a steep reverse fault produces distinctly different patterns.

What are the implications of the observed increase of effective viscosities with time, and thus stress, since the Bhuj earthquake? Such time-dependent strengthening has been observed following a number of recent large earthquakes (see overview in Bürgmann and Dresen, 2008). This behavior is predicted for flow by dislocation creep in the mantle, where strain rate is a function of stress to a power $n=3-6$ (i.e., a power-law rheology, Freed and Bürgmann, 2004). However, time-dependent viscosities are also predicted by models involving a transient rheology and can reflect a transition from early rapid relaxation by transient creep to steady-state flow (Pollitz, 2003; Hetland and Hager, 2006). The biviscous Burgers body, consisting of a Maxwell fluid and a Kelvin solid assembled in series, can be used to represent material responses with more than one relaxation time, such as might be expected for a material deforming by transient creep or a nonlinear flow law (Pollitz, 2003). If the postseismic viscous flow following the Bhuj earthquake and other short-term loading events occurs in the transient creep regime, or in the transition from transient to steady-state flow, the effective viscosities found may underestimate those relevant for long-term geodynamic processes by a factor of 2–5 based on experiments of transient dislocation creep of olivine rocks by Chopra (1997). As both the temperature and stress dependence of transient creep are found to be similar to values at steady state (Chopra, 1997), suggesting common deformation mechanisms in both regimes, it appears difficult to separate non-linear viscosity from transient creep effects in postseismic deformation studies (Handy et al., 2007). In either case, effective viscosities found in such studies probably provide only lower bounds for the long-term strength of the lithosphere.

The inferred viscosity structure can be compared with that found from post-loading studies conducted in tectonically active plate boundary regions and in stable continental interiors (see compilation of viscosity estimates in Bürgmann and Dresen (2008), their Table S2). Surprisingly, the viscosity of the upper mantle below the Bhuj region is closer to that found for thermally weakened and hydrated mantle below western North America and other back-arc or former back-arc regions (viscosity estimates generally range from $0.1–1\times10^{19}$ Pa s below 40–60 km depth) than that found from ice-unloading studies over the North American and Fennoscandian cratons (ranging from $0.5–1\times10^{21}$ Pa s below a >100-km-thick elastic lithosphere).

The low mantle viscosity deduced from the postseismic deformation may be the result of thermal weakening due to the late Cretaceous Reunion (Deccan) plume, which may also be indicated by a ~200-km-wide seismic wave speed anomaly in the uppermost mantle beneath the region (Kennett and Widiyantoro, 1999) (see inset map of Fig. 1). In contrast, the apparent strength of the lower crust is consistent with a mafic and dry composition indicated by unusually high seismic velocities at lower crustal depths (Mandal and Pujol, 2006), which may have developed in association with intrusive activity during an early Jurassic period of rifting (Chandrasekhar and Mishra, 2002). A strong lower crust is also indicated by the occurrence of earthquakes throughout the thickness of the crust (Negishi et al., 2002). Additional heat-flow measurements and seismic tomography studies in the epicentral region would be useful to better resolve the inferred variations in temperature, composition and strength of the lithosphere.

The mantle lithosphere in the Gujarat region in NW India appears to be weaker than that of fully intact continental shields. Relaxation of remote stresses in such a weak zone can concentrate stress in the overlying crust (Kenner and Segall, 2000) and lead to the observed intraplate seismicity in this region.

Acknowledgements

This study was accomplished while DC was visiting researcher at the University of California, Berkeley, USA, funded by the Department of Science and Technology, New Delhi through a BOYSCAST-Fellowship. RB acknowledges support by NSF Grant EAR-0738298. SAR data was obtained from ESA through Data Grant A03-330. We acknowledge thoughtful comments by two anonymous reviewers and stimulating discussions with Wayne Thatcher, Greg Hirth and Fred Pollitz. Berkeley Seismological Laboratory Contribution # 09-03.

Appendix A. Supplementary data

Supplementary data associated with this article can be found, in the online version, at doi:10.1016/j.epsl.2009.01.039.

References

Antolik, M., Dreger, D., 2003. Rupture process of the 26 January 2001 Mw 7.6 Bhuj, India, earthquake from teleseismic broadband data. Bull. Seismol. Soc. Am. 93, 1235–1248.
Biswas, S.K., 1987. Regional tectonic framework, structure and evolution of the western marginal basins of India. Tectonophysics 135, 302–327.
Bürgmann, R., Dresen, G., 2008. Rheology of the lower crust and upper mantle: evidence from rock mechanics, geodesy and field observations. Ann. Rev. Earth Plan. Sci. 36, 531–567.
Chandrasekhar, D.V., Mishra, D.C., 2002. Some geodynamic aspects of Kutch basin and seismicity: an insight from gravity studies. Current Science 83, 492–498.
Chandrasekhar, D.V., Mishra, D.C., Singh, B., Vijayakumar, V., Bürgmann, R., 2004. Source parameters of the Bhuj earthquake, India of January 26, 2001 from height and gravity changes. Geophys. Res. Lett. 31. doi:10.1029/2004GL020768.
Chopra, P.N., 1997. High-temperature transient creep in olivine rocks. Tectonophysics 279, 93–111.
Freed, A.M., Bürgmann, R., 2004. Evidence of powerlaw flow in the Mojave desert mantle. Nature 430, 548–551.
Handy, M.R., Hirth, G., Bürgmann, R., 2007. Continental fault structure and rheology from the frictional-to-viscous transition downward. In: Handy, M.R., et al. (Ed.), Tectonic Faults: Agents of Change on a Dynamic Earth. MIT Press, Cambridge, MA, pp. 139–181.
Haskell, N.A., 1935. The motion of a fluid under a surface load. Physics 6, 256.
Hetland, E.A., Hager, B.H., 2006. The effects of rheological layering on post-seismic deformation. Geophys. J. Int. 166. doi:10.1111/j.1365-1246X.2006.02974.x.
Jónsson, S., Segall, P., Pedersen, R., Björnsson, G., 2003. Post-earthquake ground movements correlated to pore-pressure transients. Nature 4242, 179–183.
Kenner, S., Segall, P., 2000. A mechanical model for intraplate earthquakes: application to the New Madrid Seismic Zone. Science 289, 2329–2332.
Kennett, B.L.N., Widiyantoro, S., 1999. A low seismic wavespeed anomaly beneath northwestern India: a seismic signature of the Deccan Plume? Earth Planet. Sci. Lett. 165, 145–155.
Mandal, P., Pujol, J., 2006. Seismic imaging of the aftershock zone of the 2001 Mw 7.7 Bhuj earthquake, India. Geophys. Res. Lett. 33, 1–4.
Milne, G.A., Davis, J.L., Mitrovica, J.X., Scherneck, H.G., Johansson, J.M., Vermeer, M., Koivula, H., 2001. Space-geodetic constraints on glacial isostatic adjustment in Fennoscandia. Science 291, 2381–2385.
Negishi, H., Mori, J., Sato, T., Singh, R., Kumar, S., Hirata, N., 2002. Size and orientation of the fault plane for the 2001 Gujarat, India earthquake (Mw7.7) from aftershock observations: a high stress drop event. Geophys. Res. Lett. 29. doi:10.1029/2002GL015280.
Nishimura, T., Thatcher, W., 2003. Rheology of the lithosphere inferred from postseismic uplift following the 1959 Hebgen Lake earthquake. J. Geophys. Res. 108. doi:10.1029/2002JB002191.
Okada, Y., 1985. Surface deformation due to shear and tensile faults in a half-space. Bull. Seism. Soc. Am. 75, 1135–1154.
Peltzer, G., Rosen, P., Rogez, F., Hudnut, K., 1996. Postseismic rebound in fault step-overs caused by pore fluid flow. Science 273, 1202–1204.
Pollitz, F.F., 1992. Postseismic relaxation theory on the spherical earth. Bull. Seism. Soc. Am. 82, 422–453.
Pollitz, F.F., 1997. Gravitational viscoelastic postseismic relaxation on a layered spherical Earth. J .Geophys. Res. 102, 17921–17941.
Pollitz, F.F., 2003. Transient rheology of the uppermost mantle beneath the Mojave Desert, California. Earth Planet. Sci. Lett. 215, 89–104.
Reddy, C.D., Sunil, P.S., 2008. Post-seismic crustal deformation and strain rate in Bhuj region, western India, after the 2001 January 26 earthquake. Geophys. J. Int. 172, 593–606. doi:10.1111/j.1365-1246X.2007.03641.x.
Sarkar, D., Reddy, P.R., Sain, K., Mooney, W.D., Catchings, R.D., 2001. Kutch seismicity and crustal structure. Geol. Soc. Am. Programs 262.
Schmidt, D.A., Bürgmann, R., 2006. InSAR constraints on the source parameters of the 2001Bhuj earthquake. Geophys. Res. Lett. 33. doi:10.1029/2005GL025109.
Tabei, T., 1989. Crustal movements in the inner zone of southwest Japan associated with stress relaxation after major earthquakes. J. Phys. Earth 37, 101–131.
Thatcher, W., Matsuda, T., Kato, T., Rundle, J.B., 1980. Lithospheric loading by the 1896 Riku-u earthquake, northern Japan: implication for plate flexure and asthenosphere rheology. J. Geophys. Res. 85, 6429–6435.
Wallace, K., Bilham, R., Blume, F., Gaur, V.K., Gahalaut, V.K., 2006. Geodetic constraints on the Bhuj 2001 earthquake and surface deformation in the Kachchh Rift Basin. Geophys. Res. Lett. 33. doi:10.1029/2006GL025775.
Wesnousky, S.G., Seeber, L., Rockwell, K.T., Thakur, V., Briggs, R., Kumar, S., Ragona, D., 2001. Eight days in Bhuj: field report bearing on surface rupture and genesis of the January 26, 2001 Republic Day earthquake of India. Seismol. Res. Lett. 72, 514–524.

Weak Mantle in NW India Probed by Geodetic Measurements Following the 2001 Bhuj Earthquake

D. V. Chandrasekhar[1], Roland Bürgmann[2*], C. D. Reddy[3], P. S. Sunil[3] and David Schmidt[4]

1. National Geophysical Research Institute, Hyderabad, India.

2.[*] Department of Earth and Planetary Science, University of California, Berkeley, USA.

3. Indian Institute of Geomagnetism, Mumbai, India.

4. Department of Geological Sciences, University of Oregon, Eugene, USA.

Supplementary Information

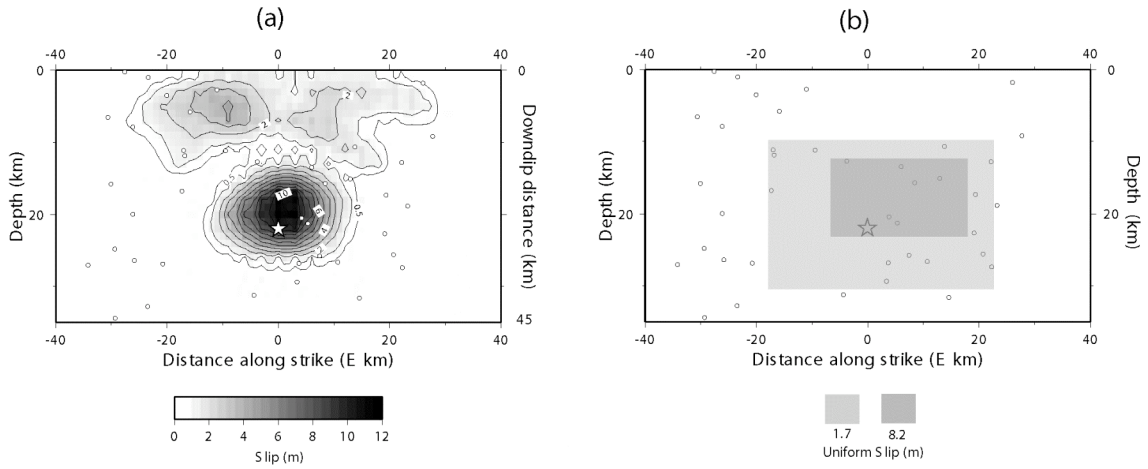

Figure S1: Source model. (a) Slip distributions for the Bhuj earthquake obtained from the broadband finite-fault inversion (Antolik and Dreger, 2003). Contoured slip amplitudes are shown as a function of distance along strike (*x* axis) and vertical depth and down-dip distance along the fault plane (y axis). The star shows the hypocenter location, and the small circles are the locations of large aftershocks. (b) The source model is simplified by compacting the slip distribution with a larger amount of slip (8.2 m) confined to the center (25 x 15 km^2) and less slip (1.7 m) on the surrounding part and used for postseismic model.

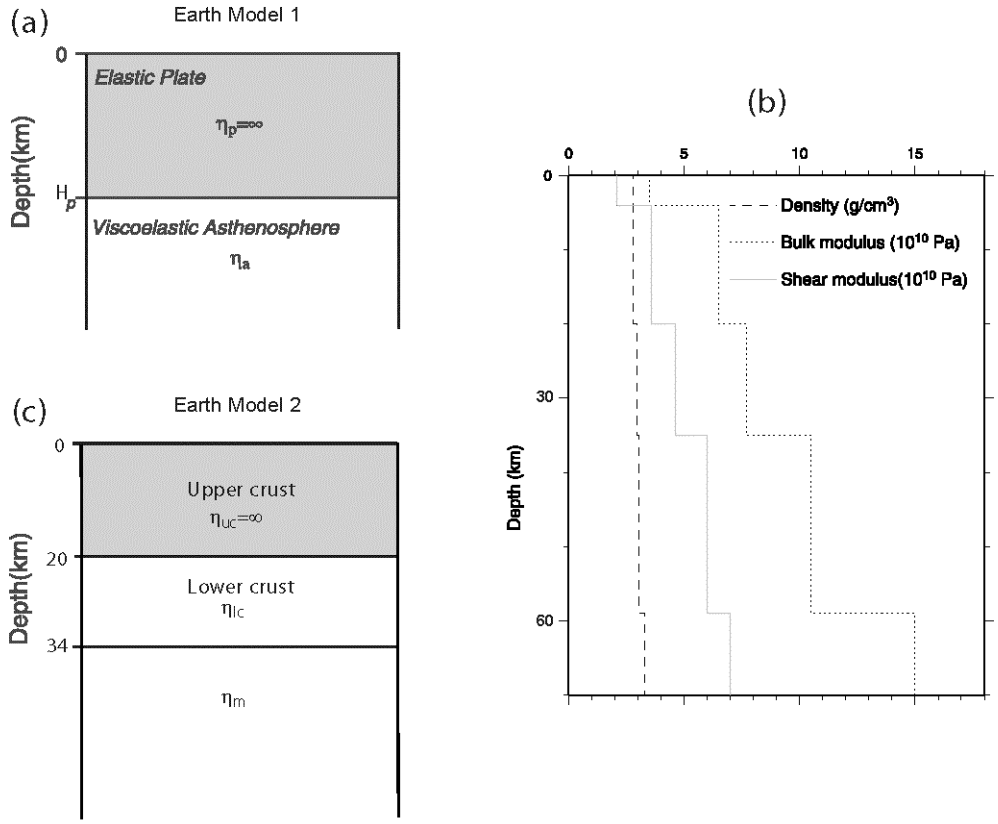

Figure S2: Layered model Earth structure. Elastic modulus and viscosity of the layered spherical Earth models. Gray areas are purely elastic. (a) Viscosity and depth of layers of the Earth model-1. (b) Shear modulus (μ), bulk modulus (κ), and density (ρ) in units of 10^{10} Pa, 10^{10} Pa, and g/cm^3 of the two-layer model. (c) Viscosity and depth of layers of the three-layer model.

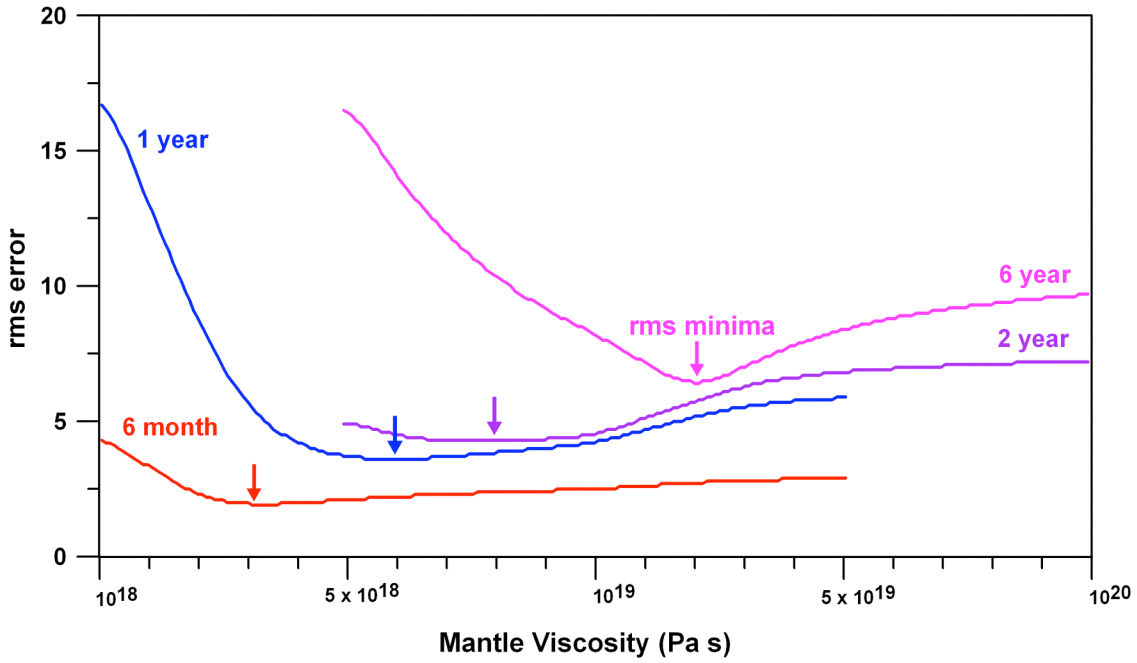

Figure S3: Plot of rms misfit as a function of mantle viscosity. Deformation in the first 6 months is better fit by a reduced effective viscosity of 3 x 10^{18} Pa s, 1 yr fit by 6 x 10^{18}, 2 yr by 8 x 10^{18} and 6 yr by 2 x 10^{19} Pa s, consistent with a time and stress dependent (e.g., power law) rheology of the upper mantle.

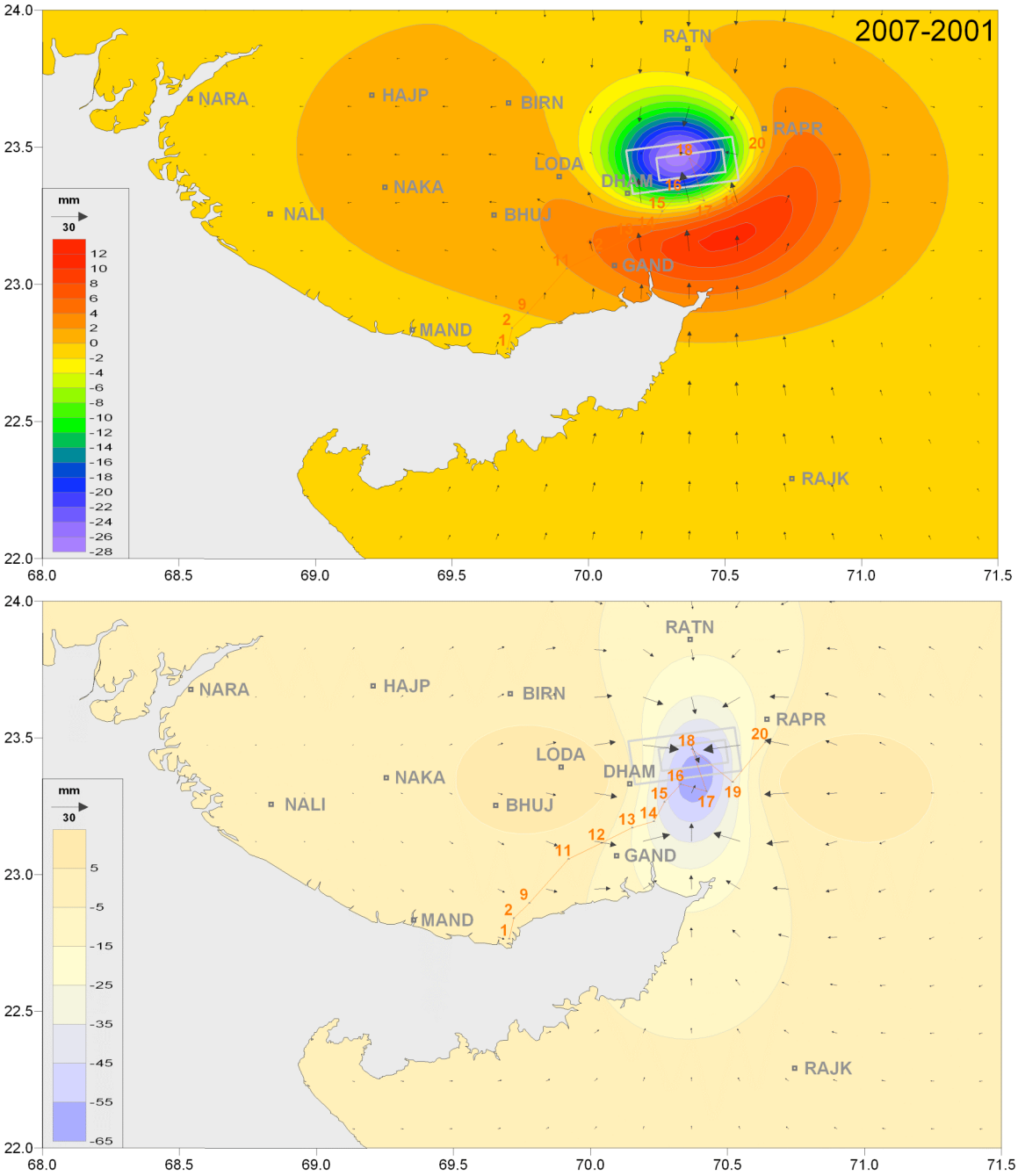

Figure S4: Poro-elastic rebound model. Comparison of the horizontal and vertical displacement field from 6 years of visco-elastic relaxation (top panel) with that predicted from poro-elastic rebound (lower panel). The pore pressure transient (Horizontal displacement as vectors and vertical displacement as contours) is shown for a typical Poisson's ratio yield (0.05) between drained and undrained materials at the hypocentral depth of the Bhuj earthquake. As this is a first order half-space calculation allowing for complete pressure equilibration at all depths, far-field motions may be overestimated.

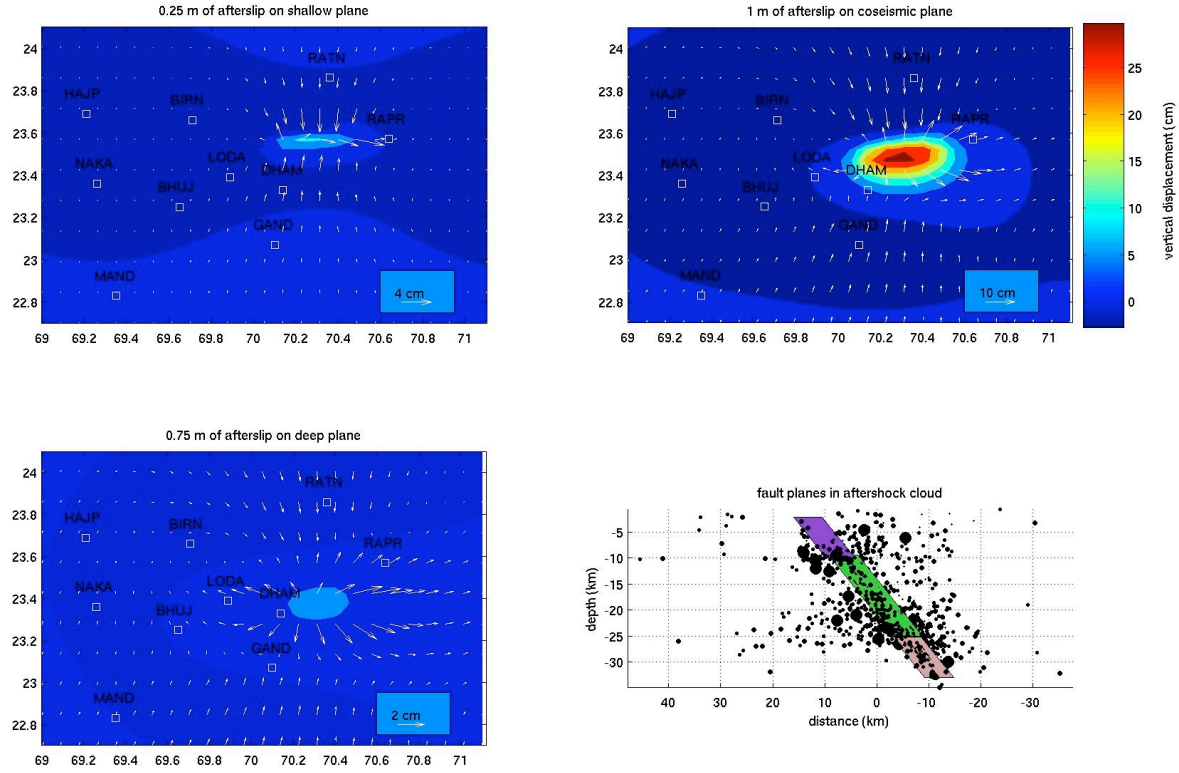

Figure S5: Afterslip models. Horizontal and vertical displacement field from first-order elastic dislocation models of afterslip updip, on, and downdip of the buried coseismic rupture of the Bhuj earthquake, respectively. The lower right panel shows the depth extent of the slip planes. Strike, dip and rake of the afterslip is assumed to be same as that in the earthquake. None of these models produce the pattern of westward motion of the western sites in the network and only shallow afterslip moves station DHAM to the north, whose early, rapid motion is not well represented by the viscoelastic model.